
Article:
Cammarano, A., Hill, T.L., Neild, S.A. et al. (2014) Bifurcations of backbone curves for systems of coupled nonlinear two mass oscillator. Nonlinear Dynamics, 77 (1-2). 311 - 320. ISSN: 0924-090X

https://doi.org/10.1007/s11071-014-1295-3

Nonlinear Dynamics manuscript No.
(will be inserted by the editor)

Bifurcations of backbone curves for systems of coupled nonlinear two mass oscillator

A. Cammarano · T.L. Hill · S.A. Neild · D.J. Wagg

Received: date / Accepted: date

Abstract This paper considers the dynamic response of coupled, forced and lightly damped nonlinear oscillators with two degree-of-freedom. For these systems, backbone curves define the resonant peaks in the frequency–displacement plane and give valuable information on the prediction of the frequency response of the system.

Previously, it has been shown that bifurcations can occur in the backbone curves. In this paper we present an analytical method enabling the identification of the conditions under which such bifurcations occur. The method, based on second order nonlinear normal forms, is also able to provide information on the nature of the bifurcations and how they affect the characteristics of the response.

This approach is applied to a two-degree-of-freedom mass, spring, damper system with cubic hardening springs. We use the second-order normal form method to transform the system coordinates and identify which parameter values will lead to resonant interactions and bifurcations of the backbone curves. Furthermore, the relationship between the backbone curves and the complex dynamics of the forced system is shown.

Keywords Backbone curve · Bifurcation · Nonlinear oscillator · Second-order normal form method

A. Cammarano
Department of Mechanical Engineering, University of Bristol, Bristol, BS8 1TR, UK
Tel.: +44 (0) 784 656 6489
E-mail: andrea.cammarano@bristol.ac.uk

T.L. Hill
Department of Mechanical Engineering, University of Bristol, Bristol, BS8 1TR, UK

S.A. Neild
Department of Mechanical Engineering, University of Bristol, Bristol, BS8 1TR, UK

D.J. Wagg
Department of Mechanical Engineering, University of Sheffield, Sheffield S1 3JD, UK

1 Introduction

Many vibration problems in engineering concern forced, lightly damped and weakly nonlinear multi-degree-of-freedom (MDOF) systems. In these systems, resonant peaks are typically observed in the frequency response. This paper considers the response of such systems, and how they can be described in terms of interactions between the resonances. Many authors have considered problems of this type, although the majority have considered the case of single-degree-of-freedom nonlinear oscillators. Background material on coupled, forced oscillators can be found in [1–6].

Backbone curves describe the behaviour of the underlying Hamiltonian systems (i.e. when the systems are unforced and undamped), and relate directly to the behaviour of the forced systems. As a result the backbone curves can be used to extract information about the shape and location of the peaks in the frequency response. Here the second-order normal form technique proposed by [7] for MDOF systems is used to identify resonant interactions and develop analytical expressions for the backbone curves. Particular attention is paid to the bifurcation of the backbone curves and their significance.

Lewandowski [8] first pointed out that bifurcations can occur in the backbone curves of a two-mode model applied to the free vibration of an undamped, unforced beam with axial loading. The same author analysed beams, membranes and plate structures using the same two-mode model approach, derived using a Galerkin decomposition [9].

Lewandowski defined *primary* (or first non-trivial) bifurcation points as those at which the trivial solutions lose stability. Trivial solutions are those where displacement amplitudes equal zero, therefore they are also known as *zero solutions*. In the plane of forcing frequency vs. displacement amplitude, these points occur at the linearised natural frequencies and form the first points on what Lewandowski called the fundamental backbone curve. *Secondary* bifurcation points are those which exist on the fundamental backbone curve where displacement amplitudes are non-zero.

The second-order normal forms reduces the dynamics of a system to a set of time-independent algebraic equations. This provides analytical expressions for the backbone curves which can be used to define the conditions for which the bifurcations occur, giving valuable insight into the relationship between the physical characteristics of a system and its response.

The use of the normal form analysis offers several advantages over the approach taken by Lewandowski. Most notably it (i) allows phase dependence between the two backbone curve solutions to be quantified, (ii) identifies all the potential internal resonances for the system being considered, and finally (iii) relates the backbone curves to the forced, damped response.

After a general description of the method, the normal form approach is demonstrated using a two-degree-of-freedom mass, spring, damper system, with the masses coupled by a cubic spring. This system has been studied in the context of bifurcating nonlinear normal modes [10] and localisation [11–13], in which the example discussed has a special symmetry achieved when

the coupling spring has no linear stiffness. This means that the primary and secondary bifurcation points, as defined by Lewandowski, are coincident. The special symmetry in [11,12] is essential in order to derive simple analytical expressions. The more general case, where the coupling is via a spring with both linear and cubic stiffness, was considered by [6]. It is this generalised case that we consider here. In addition we are predominantly interested in the secondary bifurcations and the subsequent dynamical behaviour.

After a brief description of the method in Section 2, the analysis of the two-mass system with nonlinear stiffness is presented in Section 3. Finally, after discussion of how the backbone curves describe the underlying dynamics of the forced response in Section 4, conclusions are drawn in Section 5.

2 Analytical methods

In this section a brief description of the second-order normal form technique [7] (a variation of the more common first-order normal form [14,15]), used for the derivation of the backbone curves, is provided. Here the method is presented in its most general formulation; however detailed discussions are given in [16, 17]. This approach can give valuable insight into the physics of the observed behaviour, as will be seen in Section 3.

While it is possible to conduct the analysis shown here using other approximate analytical methods, we select the second-order normal form technique due to its matrix formulation which allows more convenient straightforward computation. In addition, the homological equation which arises in the method can be used to easily identify resonant interactions between the backbone curves. The method consists of three transforms:

- A linear modal transform – the system is projected onto the linear modes (i.e. the modes of the underlying linear system). Note that throughout this paper, the term *mode* refers to the projection onto the linear modes.
- A forcing transform – this removes, from each modal equation of motion, any forcing terms that are not close to the natural frequency.
- A nonlinear near-identity transform – this removes any non-resonant terms from each equation of motion.

Once these transforms are applied, each mode is described by an equation of motion consisting only of the terms resonating at one frequency — the response frequency (ω_{ri} for the i^{th} mode). This allows the harmonic components to be balanced, removing any time-dependence and enabling a solution to be found relatively easily. For the sake of clarity we point out that the frequency at which the i^{th} mode responds is named here as ω_{ri}, whereas the i^{th} underlying linear natural frequency is denoted ω_{ni}.

The first two transforms are not presented as the linear modal transform is straightforward and the forcing transform is unity, as the backbone curves describe the unforced system. Broadly adopting the notation used by [17], we

write the resulting unforced modal dynamics as

$$\ddot{\mathbf{v}} + \mathbf{\Lambda}\mathbf{v} + \mathbf{N}_v(\mathbf{v}, \dot{\mathbf{v}}) = 0, \tag{1}$$

where $\mathbf{v}$ is a vector of modal displacements, $\mathbf{\Lambda}$ is a diagonal matrix where the i^{th} diagonal term is ω_{ni}^2 and $\mathbf{N}_v$ contains the nonlinear coupling terms, which are assumed to be small. The final step in the technique is the near-identity nonlinear transform $\mathbf{v} \to \mathbf{u}$

$$\begin{array}{c} \mathbf{v} = \mathbf{u} + \mathbf{H}(\mathbf{u}, \dot{\mathbf{u}}) \\ \ddot{\mathbf{v}} + \mathbf{\Lambda}\mathbf{v} + \mathbf{N}_v(\mathbf{v}, \dot{\mathbf{v}}) = 0 \qquad \longrightarrow \qquad \ddot{\mathbf{u}} + \mathbf{\Lambda}\mathbf{u} + \mathbf{N}_u(\mathbf{u}, \dot{\mathbf{u}}) = 0, \end{array} \tag{2}$$

where $\mathbf{H}$ is used to store terms that do not contribute to the fundamental response. Meanwhile, all nonlinear terms resonating at ω_{ri}, for the i^{th} mode, are captured in $\mathbf{N}_u$. This is distinct from the harmonic balance technique, as the non-resonant terms are not discarded and may later be combined with the fundamental response.

This then allows the equation of motion in u_i, where u_i is the i^{th} element in $\mathbf{u}$, to be solved using the solution $u_i = U_i \cos(\omega_{ri} t - \phi_i)$, where U_i is the amplitude and ϕ_i is the phase of the fundamental response of the i^{th} mode. This is more conveniently expressed as

$$u_i = u_{ip} + u_{im} = \frac{U_i}{2} \mathrm{e}^{+\mathrm{j}(\omega_{ri} t - \phi_i)} + \frac{U_i}{2} \mathrm{e}^{-\mathrm{j}(\omega_{ri} t - \phi_i)}. \tag{3}$$

To calculate $\mathbf{H}$ and $\mathbf{N}_u$, we write $\mathbf{N}_v$ in the form

$$\mathbf{N}_v(\mathbf{u}, \dot{\mathbf{u}}) = \mathbf{n}_v \mathbf{u}^*(\mathbf{u}_p, \mathbf{u}_m), \tag{4}$$

where $\mathbf{u}^*$ is a column vector containing all the combinations of variables in terms that appear in $\mathbf{N}_v$ after the substitution $u_i = u_{ip} + u_{im}$ has been made. In general, for a system with I modes, the ℓ^{th} element is given by

$$u_\ell^* = \prod_{i=1}^{I} \left\{ u_{ip}^{s_{\ell ip}} u_{im}^{s_{\ell im}} \right\}, \tag{5}$$

which may be used to define $s_{\ell ip}$ and $s_{\ell im}$ – the exponents of u_{ip} and u_{im} respectively. Following the form of Eq. (4), we define

$$\mathbf{N}_u(\mathbf{u}, \dot{\mathbf{u}}) = \mathbf{n}_u \mathbf{u}^*(\mathbf{u}_p, \mathbf{u}_m), \tag{6}$$

$$\mathbf{H}(\mathbf{u}, \dot{\mathbf{u}}) = \mathbf{h}\mathbf{u}^*(\mathbf{u}_p, \mathbf{u}_m). \tag{7}$$

It is common to define a book-keeping parameter ε which is associated with small terms, such as the nonlinear ones, to allow us to track the order of "smallness" of the subsequent terms, see for example [18]. Here we simply neglect terms that are generated from the product of small terms, as these are of order ε^2 and above.

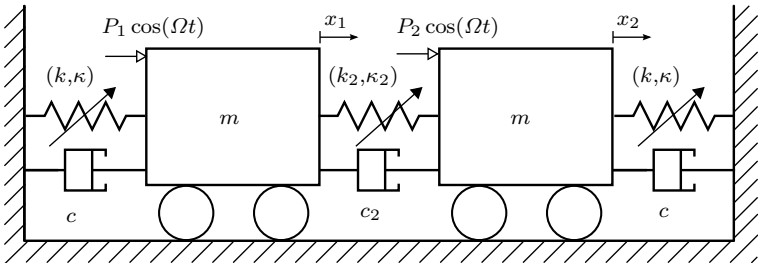

Fig. 1: A schematic diagram of a two-mass oscillator with a symmetric structure.

By substituting the transform equation, $\mathbf{v} = \mathbf{u} + \mathbf{H}$, into the dynamic equation for $\mathbf{v}$, Eq. (2), and comparing to that for $\mathbf{u}$, to order ε^1 we find the relationship

$$n_{v,i\ell} = n_{u,i\ell} + \beta_{i\ell} h_{i\ell}, \tag{8}$$

where $n_{v,i\ell}$ is element $\{i,\ell\}$ of $\mathbf{n}_v$ etc, corresponding to the i^{th} mode and ℓ^{th} element in $\mathbf{u}^*$, and $\beta_{i\ell}$ (element $\{i,\ell\}$ of a matrix $\boldsymbol{\beta}$) is given by

$$\beta_{i\ell} = \left[\sum_{k=1}^{I} (s_{\ell kp} - s_{\ell km})\omega_{rk}\right]^2 - \omega_{ri}^2, \tag{9}$$

where we have used the general representation for the ℓ^{th} term in $\mathbf{u}^*$, see Eq. (5).

Equation (8) represents a choice, as there is just one equation to find the two unknowns $n_{u,i\ell}$ and $h_{i\ell}$. To keep the equation of motion simple it is desirable to set $n_{u,i\ell} = 0$, such that $h_{i\ell} = n_{v,i\ell}/\beta_{i\ell}$, where possible. However the technique relies on the transform $\mathbf{v} = \mathbf{u} + \mathbf{H}$ being near-identity (such that $\mathbf{H}$ is order ε^1). For the case where $\beta_{i\ell}$ is small, or zero, this cannot be achieved while setting $h_{i\ell} = n_{v,i\ell}/\beta_{i\ell}$. Hence, when $\beta_{i\ell}$ is zero (or small) we set $n_{u,i\ell} = n_{v,i\ell}$ and $h_{i\ell} = 0$, and these terms are referred to as the resonant (or near-resonant) terms respectively.

Having identified the resonant terms, the transformed equation for the dynamics in terms of $\mathbf{u}$ (see Eq. (2)) can be found. The solution to this may be found by substituting for u_i using Eq. (3) allowing time-independent expressions in terms of modal amplitude and phase to be obtained. These expressions can then be used to identify the backbone curves. We will demonstrate this in the next section with the aid of an example.

3 A two-degree-of-freedom system

We now consider a two-mass oscillator with a symmetric structure, as shown in Figure 1. Identical springs, with force-deflection relationships $F = k(\Delta x) +$

$\kappa(\Delta x)^3$, connect the two masses to ground and another spring, with a force-deflection relationship $F_2 = k_2(\Delta x) + \kappa_2(\Delta x)^3$, connects the two masses. We assume that the springs are stiffening, such that κ and κ_2 are positive. Linear viscous dampers also connect the masses to ground (damping c) and to each other (damping c_2). The first and second masses (both of mass m) are subjected to the sinusoidal forcing $P_1\cos(\Omega t)$ and $P_2\cos(\Omega t)$ respectively.

3.1 Backbone curves

The equation of motion of this system, expressed in linear modal coordinates (see Eq. (1)) using modeshapes $\{x_1,\ x_2\}^T = \{1,\ 1\}^T$ and $\{x_1,\ x_2\}^T = \{1,\ -1\}^T$ for the first and second mode respectively, is

$$\ddot{\mathbf{v}} + \mathbf{\Lambda}\mathbf{v} + \mathbf{N}_v = \mathbf{P}_v \quad \text{where:} \tag{10}$$
$$\mathbf{N}_v = \frac{\kappa}{m}\begin{pmatrix} v_1^3 + 3v_1v_2^2 \\ 3v_1^2v_2 + \gamma v_2^3 \end{pmatrix} + \begin{bmatrix} 2\zeta_1\omega_{n1} & 0 \\ 0 & 2\zeta_2\omega_{n2} \end{bmatrix}\dot{\mathbf{v}},$$
$$\mathbf{P}_v = \frac{1}{2\,m}\begin{pmatrix} P_1 + P_2 \\ P_1 - P_2 \end{pmatrix}\cos(\Omega t).$$

In this equation we have also included modal damping and external forcing terms, which we later use when simulating the full system. In addition, here $\gamma = 1 + (8\kappa_2/\kappa)$, $2\zeta_1\omega_{n1} = c/m$, $2\zeta_2\omega_{n2} = (c + 2c_2)/m$ and $\mathbf{\Lambda}$ is a diagonal matrix of the squares of the linear natural frequencies $\omega_{n1}^2 = k/m$ and $\omega_{n2}^2 = (k + 2k_2)/m$. For convenience, we define modal forcing amplitudes in terms of the equivalent linear system P_{m1} and P_{m2} such that

$$\mathbf{P}_v = \begin{pmatrix} P_{m1} \\ P_{m2} \end{pmatrix}\cos(\Omega t), \tag{11}$$

i.e. $P_{m1} = P_1 + P_2$ and $P_{m2} = P_1 - P_2$.

The backbone curves give the underlying structure of the amplitude of displacement response at ω_{ri} by considering the unforced, undamped system, which for this example is

$$\ddot{\mathbf{v}} + \mathbf{\Lambda}\mathbf{v} + \frac{\kappa}{m}\begin{pmatrix} v_1^3 + 3v_1v_2^2 \\ 3v_1^2v_2 + \gamma v_2^3 \end{pmatrix} = 0. \tag{12}$$

For convenience we now define r as the ratio between the response frequencies, such that $\omega_{r2} = r\omega_{r1}$. Using this, the nonlinear terms can be rewritten in the form of Eq. (4) and the corresponding $\boldsymbol{\beta}$ matrix can be calculated using

Eq. (9) giving

$$\mathbf{u}^* = \begin{bmatrix} u_{1p}^3 \\ u_{1p}^2 u_{1m} \\ u_{1p} u_{1m}^2 \\ u_{1m}^3 \\ u_{1p} u_{2p}^2 \\ u_{1p} u_{2p} u_{2m} \\ u_{1p} u_{2m}^2 \\ u_{1m} u_{2p}^2 \\ u_{1m} u_{2p} u_{2m} \\ u_{1m} u_{2m}^2 \\ u_{1p}^2 u_{2p} \\ u_{1p}^2 u_{2m} \\ u_{1p} u_{1m} u_{2p} \\ u_{1p} u_{1m} u_{2m} \\ u_{1m}^2 u_{2p} \\ u_{1m}^2 u_{2m} \\ u_{2p}^3 \\ u_{2p}^2 u_{2m} \\ u_{2p} u_{2m}^2 \\ u_{2m}^3 \end{bmatrix}, \quad \mathbf{n}_v^T = \frac{\kappa}{m} \begin{bmatrix} 1 & 0 \\ 3 & 0 \\ 3 & 0 \\ 1 & 0 \\ 3 & 0 \\ 6 & 0 \\ 3 & 0 \\ 3 & 0 \\ 6 & 0 \\ 3 & 0 \\ 0 & 3 \\ 0 & 3 \\ 0 & 6 \\ 0 & 6 \\ 0 & 3 \\ 0 & 3 \\ 0 & \gamma \\ 0 & 3\gamma \\ 0 & 3\gamma \\ 0 & \gamma \end{bmatrix}, \quad \boldsymbol{\beta}^T = \omega_{r1}^2 \begin{bmatrix} 8 & - \\ 0 & - \\ 0 & - \\ 8 & - \\ 4(r^2+r) & - \\ 0 & - \\ 4(r^2-r) & - \\ 4(r^2-r) & - \\ 0 & - \\ 4(r^2+r) & - \\ - & 4(1+r) \\ - & 4(1-r) \\ - & 0 \\ - & 0 \\ - & 4(1-r) \\ - & 4(1+r) \\ - & 8r^2 \\ - & 0 \\ - & 0 \\ - & 8r^2 \end{bmatrix},$$

where, in $\boldsymbol{\beta}$, a dash has been used where the corresponding value in $\mathbf{n}_v$ is zero and hence the value in $\boldsymbol{\beta}$ is of no importance. The resonant terms in $\mathbf{n}_v$ are identified as those corresponding to terms in $\boldsymbol{\beta}$ with a value of zero. These fall into two categories: those which are zero regardless of the value of r, which we call the *unconditionally-resonant* terms; and those which are zero for a specific value of r, which we call the *conditionally-resonant* terms.

For all resonant terms we set the corresponding terms in $\mathbf{n}_u$ as equal to those in $\mathbf{n}_v$. The resulting dynamic equations are

$$\ddot{u}_1 + \omega_{n1}^2 u_1 + \frac{3\kappa}{m}\left[u_{1p}u_{1m}u_1 + 2u_{2p}u_{2m}u_1 + \delta(r-1)(u_{1p}u_{2m}^2 + u_{1m}u_{2p}^2)\right] = 0, \tag{13a}$$

$$\ddot{u}_2 + \omega_{n2}^2 u_2 + \frac{3\kappa}{m}\left[\gamma u_{2p}u_{2m}u_2 + 2u_{1p}u_{1m}u_2 + \delta(r-1)(u_{1p}^2 u_{2m} + u_{1m}^2 u_{2p})\right] = 0, \tag{13b}$$

where $u_i = u_{ip} + u_{im}$, Eq. (3), has been used and δ is the Dirac-delta function. Making the substitutions $u_{ip} = (U_i/2)\mathrm{e}^{+\mathrm{j}(\omega_{ri}t-\phi_i)}$ and $u_{im} = (U_i/2)\mathrm{e}^{-\mathrm{j}(\omega_{ri}t-\phi_i)}$, we can write Eqs. (13) in the form

$$\chi_i \mathrm{e}^{+\mathrm{j}\omega_{ri}t} + \tilde{\chi}_i \mathrm{e}^{-\mathrm{j}\omega_{ri}t} = 0, \tag{14}$$

where χ_i and $\tilde{\chi}_i$ are complex conjugates. Inspecting the components of Eqs. (13) corresponding to χ_i, and noting that $\omega_{r2} = r\omega_{r1}$, leads to the time-independent

equations

$$\left[-\omega_{r1}^2+\omega_{n1}^2+\frac{3\kappa}{4m}\left\{U_1^2+U_2^2\left(2+\delta(r-1)\mathrm{e}^{+\mathrm{j}2(\phi_1-\phi_2)}\right)\right\}\right]U_1=0, \quad (15a)$$

$$\left[-r^2\omega_{r1}^2+\omega_{n2}^2+\frac{3\kappa}{4m}\left\{\gamma U_2^2+U_1^2\left(2+\delta(r-1)\mathrm{e}^{-\mathrm{j}2(\phi_1-\phi_2)}\right)\right\}\right]U_2=0. \quad (15b)$$

There are two straightforward solutions to Eqs. (15) which can be found by setting U_1 and then U_2 to zero. These single-mode responses describe the backbone curves *S1* and *S2* as

$$S1\text{:}\ \ U_2=0,\ \ \omega_{r1}^2=\omega_{n1}^2+\frac{3\kappa}{4m}U_1^2, \quad (16)$$

$$S2\text{:}\ \ U_1=0,\ \ \omega_{r2}^2=\omega_{n2}^2+\frac{3\kappa\gamma}{4m}U_2^2. \quad (17)$$

Solutions in which both modes are present are also possible if both expressions in the square brackets in Eqs. (15) are zero. Considering this, if $r\neq 1$ only unconditionally-resonant terms are present in the expressions. These terms do result in coupling between the modes however this coupling is only by amplitude and not by phase. Phase-independence between modes indicates their interaction is non-resonant.

For the special case where $r=1$, conditionally-resonant terms (the terms multiplied by $\delta(r-1)$) are also present. These terms do result in phase-dependence, leading to a resonant response with modal cross-coupling. It is the $r=1$ case that we now consider, which is achieved by setting $k_2 \ll k$ such that ω_{n1} and ω_{n2} are close.

The imaginary parts of Eqs. (15) lead to $\sin(2|\phi_1-\phi_2|)=0$. Hence $\mathrm{e}^{\mathrm{j}2|\phi_1-\phi_2|}=\cos(2|\phi_1-\phi_2|)=\pm 1$, and we may write

$$p=\mathrm{e}^{\mathrm{j}2|\phi_1-\phi_2|}=\pm 1, \quad (18)$$

where $p=+1$ relates to $|\phi_1-\phi_2|=0,\pi,2\pi,...$ i.e. the two modes are in-phase or anti-phase. The case $p=-1$ does not correspond to any physical solution of this system and therefore is not considered.

Following these considerations, Eqs. (15) can be arranged as

$$\left[-\omega_{r1}^2+\omega_{n1}^2+\frac{3\kappa}{4m}\left\{U_1^2+3\,U_2^2\right\}\right]U_1=0, \quad (19a)$$

$$\left[-\omega_{r1}^2+\omega_{n2}^2+\frac{3\kappa}{4m}\left\{\gamma U_2^2+3\,U_1^2)\right\}\right]U_2=0. \quad (19b)$$

In addition to the solution given in Eqs. (16) and (17), further solutions are possible by setting both expressions in the squared brackets to zero. This gives

$$\omega_{r1}^2=\omega_{n1}^2+\frac{3\kappa}{4m}\left\{U_1^2+3\,U_2^2\right\}=\omega_{n2}^2+\frac{3\kappa}{4m}\left\{\gamma U_2^2+3\,U_1^2)\right\}, \quad (20)$$

or, when rearranged

$$\frac{3\kappa}{4m}\left\{\left(2-\frac{8\kappa_2}{\kappa}\right)U_2^2-2\,U_1^2\right\}=\omega_{n2}^2-\omega_{n1}^2, \tag{21}$$

where it has been recalled that $\gamma=1+(8\kappa_2/\kappa)$.

From Eq. (21) the following expression for U_1^2 can be found

$$U_1^2=(1-4\frac{\kappa_2}{\kappa})U_2^2-\frac{2m}{3\kappa}(\omega_{n2}^2-\omega_{n1}^2). \tag{22}$$

From inspection it can be seen that, as U_1 must be real, two conditions exist

$$\kappa\geq 4\kappa_2 \quad \text{and} \quad U_2^2\geq\frac{2m}{3(\kappa-4\kappa_2)}(\omega_{n2}^2-\omega_{n1}^2), \tag{23}$$

which must both be satisfied. Manipulation of Eq. (20), using Eq. (22) to eliminate U_1^2, leads to the amplitude-frequency relation

$$\omega_{r1}^2=\omega_{r2}^2=\frac{3\omega_{n1}^2-\omega_{n2}^2}{2}+\frac{3(\kappa-\kappa_2)}{m}U_2^2. \tag{24}$$

This solution to Eqs. (19) results in two additional backbone curves, $S\mathcal{3}^+$ and $S\mathcal{3}^-$, both having the same amplitude-frequency relationship

$$S\mathcal{3}^{\pm}: \qquad U_1=\sqrt{(1-4\frac{\kappa_2}{\kappa})U_2^2-\frac{2m}{3\kappa}(\omega_{n2}^2-\omega_{n1}^2)}, \tag{25a}$$

$$\omega_{r1}^2=\frac{3\omega_{n1}^2-\omega_{n2}^2}{2}+\frac{3(\kappa-\kappa_2)}{m}U_2^2, \tag{25b}$$

but characterised by the phase differences

$$S\mathcal{3}^+: |\phi_1-\phi_2|=0, \tag{26a}$$

$$S\mathcal{3}^-: |\phi_1-\phi_2|=\pi, \tag{26b}$$

i.e. $S\mathcal{3}^+$ is an in-phase solution and $S\mathcal{3}^-$ is an anti-phase solution.

It is worth noting that when $U_1=0$, Eq. (25b) leads to $U_2^2=2m(\omega_{n2}^2-\omega_{n1}^2)/3(\kappa-4\kappa_2)$, and the response frequency equation simplifies to

$$\omega_{r2}^2=\omega_{n2}^2+\frac{3\kappa\gamma}{4m}U_2^2, \tag{27}$$

which is the same expression found for *S2*, see Eq. (17). This implies that the $S\mathcal{3}^+$ and $S\mathcal{3}^-$ meet *S2* when $U_1\to 0$. This defines a bifurcation point in the backbone curve *S2*.

From this we can see that (i) as $\kappa\to 4\kappa_2$ from above, the magnitude of U_2 at which the bifurcation occurs tends to ∞ and (ii) as $k_2\to 0$, then $\omega_{n2}\to\omega_{n1}$ and the magnitude of U_2 at which the bifurcation occurs tends to 0. This second limit corresponds to the system studied in [19], where the system behavior is presented in terms of the ratio of displacement amplitude rather than in the frequency domain.

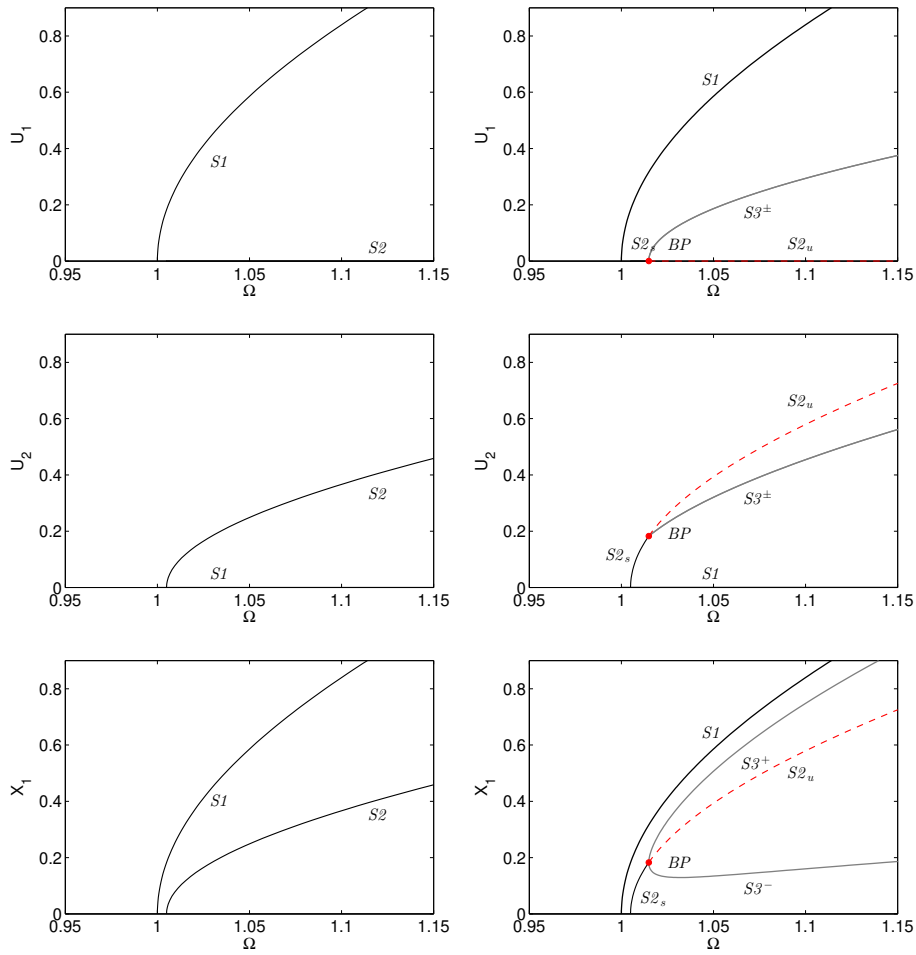

Fig. 2: Backbone curves for $\omega_{n1} = 1$, $\omega_{n2} = 1.005$, $\kappa = 0.4$. The panels in the left and the right column show the cases $\kappa_2 = 0.2$ ($\kappa < 4\kappa_2$) and $\kappa_2 = 0.05$ ($\kappa > 4\kappa_2$) respectively. In the left and right row, the projection of amplitude of the fundamental response in terms of u_1 and u_2 is shown. In the third row, the backbone curves are represented in the projection of amplitude of displacement of the first mass. Stable solutions are shown with solid black lines, whereas unstable solutions are represented by dashed red lines. Bifurcation points are indicated with red bullets labelled BP. (Strictly these are the secondary bifurcations points as defined by Lewandowski [8,9]).

Figure 2 shows the backbone curves for the cases where $\omega_{n1} = 1$, $\omega_{n2} = 1.005$, $\kappa = 0.4$. The panels in the left and right columns show the backbone curves for values $\kappa_2 = 0.2$ and $\kappa_2 = 0.05$ respectively. The left column shows the two distinct backbone curves corresponding to solutions *S1* and *S2*, see Eqs. (16) and (17). For this case $\kappa < 4\kappa_2$ and so no further real solutions exist. As $\kappa > 4\kappa_2$ in the right column, the additional solutions $S3^+$ and $S3^-$ (see Eqs. (25) and (26)) appear alongside the modified *S1* and *S2* solutions.

All panels show the backbone curves in the projection of response frequency (generalised as $\Omega = \omega_{r1} = \omega_{r2}$) against a displacement. The first and second rows show the amplitude of displacement of the fundamental response of u_1 and u_2 (i.e. U_1 and U_2 respectively). In the third row, the amplitude of displacement of the first mass is shown. This can be found by considering the contributions of u_1 and u_2 to x_1. Note that in this row, the panel on the left would show identical results, if instead, the displacement amplitude of the second mass was considered. On the other hand, in panel on the right, the branches *S1* and *S2* would be identical but $S3^+$ and $S3^-$ would be swapped. This is due to the bifurcation in *S2* breaking the symmetry between the displacement of the two masses which, for a given frequency, have different displacements amplitudes on $S3^{\pm}$.

In both cases, the approximate algebraic solutions calculated using the second-order normal form technique agree almost exactly with the backbone curves computed using the continuation software AUTO-07p [23]. Here, the numerical solutions are not shown as the error in the frequency range considered is less than 0.1% making the two solutions indistinguishable.

3.2 Stability of the backbone curves

The stability of the backbone curves can be analyzed using the solution provided by Eqs. (13). In this work only the stability of *S2* is derived, although the study may be extended to the other branches.

On the branch *S2*, as shown in top-right panel in Figure 2, u_1 is equal to zero and the solution is comprised only of u_2. As is done when deriving Arnold tongues, see for example [1], we can determine the stability of *S2* by considering the dynamics of u_1 about its zero-solution. On the *S2* branch, when the zero-solution of u_1 is unstable, the *S2* solution is also unstable.

Using Eq. (13a), for the case where $r = 1$, we have

$$\ddot{u}_1 + \omega_{n1}^2 u_1 + \frac{3\kappa}{m}\left[2u_{2p}u_{2m}u_1 + u_{1p}u_{2m}^2 + u_{1m}u_{2p}^2\right] = 0. \tag{28}$$

Since we are considering u_1 in the proximity of its zero-solution, the $u_{1p}u_{1m}u_1$ term is very small and so has been neglected. The stability is found by allowing the amplitude and phase of u_1 to be a slowly varying function of time using the parameter ε to denote "smallness". Using this we may write u_1 as

$$u_1 = u_{1p} + u_{1m} = \frac{U_{1p}(\varepsilon t)}{2}\mathrm{e}^{\mathrm{j}\omega_{r1}t} + \frac{U_{1m}(\varepsilon t)}{2}\mathrm{e}^{-\mathrm{j}\omega_{r1}t}. \tag{29}$$

Following the approach of [20], but using a complex exponential rather than trigonometric representation, we then write

$$\ddot{u}_1 = -\omega_{r1}^2 u_1 + \mathrm{j}\omega_{r1}\varepsilon\left(\frac{\dot{U}_{1p}(\varepsilon t)}{2}\mathrm{e}^{\mathrm{j}\omega_{r1}t} - \frac{\dot{U}_{1m}(\varepsilon t)}{2}\mathrm{e}^{-\mathrm{j}\omega_{r1}t}\right) + \mathcal{O}\{\varepsilon^2\}, \qquad (30)$$

where terms of order ε^2 are neglected. Substituting this expression into Eq. (28) and then balancing the $\mathrm{e}^{\mathrm{j}\omega t}$ and $\mathrm{e}^{-\mathrm{j}\omega t}$ terms gives

$$\dot{U}_{1p} = -\mathrm{j}\left(\frac{\omega_{r1}^2 - \omega_{n1}^2}{\omega_{r1}}\right)U_{1p} \; + \mathrm{j}\frac{3\kappa}{4m\omega_{r1}}\left(2U_{2m}U_{2p}U_{1p} + U_{2p}^2 U_{1m}\right), \qquad (31a)$$

$$\dot{U}_{1m} = \quad \mathrm{j}\left(\frac{\omega_{r1}^2 - \omega_{n1}^2}{\omega_{r1}}\right)U_{1m} - \mathrm{j}\frac{3\kappa}{4m\omega_{r1}}\left(2U_{2p}U_{2m}U_{1m} + U_{2m}^2 U_{1p}\right). \qquad (31b)$$

These equations can be rearranged into the form $\dot{\mathbf{U}}_1 = \mathbf{f}(U_{1p}, U_{1m}, U_{2p}, U_{2m})$, where $\mathbf{U}_1 = [U_{1p}\; U_{1m}]^T$. The stability of the zero-solution can then be assessed by considering the eigenvalues of the matrix of derivatives of $\mathbf{f}$, $\mathbf{f}_{\mathbf{U}_1}$, about the equilibrium solution $\mathbf{U}_1 = 0$, see [20], calculated from

$$\mathbf{f}_{\mathbf{U}_1} = \frac{\mathrm{j}}{\omega_{r1}}\begin{bmatrix} \frac{3\kappa}{4m}U_{2p}U_{2m} - \frac{\omega_{r1}^2-\omega_{n1}^2}{2} & \frac{3\kappa}{8m}U_{2p}^2 \\ -\frac{3\kappa}{8m}U_{2m}^2 & -\frac{3\kappa}{4m}U_{2m}U_{2p} + \frac{\omega_{r1}^2-\omega_{n1}^2}{2} \end{bmatrix}, \qquad (32)$$

The eigenvalues of $\mathbf{f}_{\mathbf{U}_1}$, λ, are given by

$$\omega_{r1}^2\lambda^2 + \left(\frac{3\kappa}{4m}U_2^2 - \frac{\omega_{r1}^2 - \omega_{n1}^2}{2}\right)^2 - \left(\frac{3\kappa}{8m}U_2^2\right)^2 = 0, \qquad (33)$$

where $U_2^2 = U_{2p}U_{2m}$ has been used.

Two possible conditions can be determined from the roots of this equation: when the roots are both purely imaginary the system is marginally stable, when the roots are real the system is unstable. This implies that the bifurcation point occurs when the roots are both zero, i.e. when

$$\left|\frac{3\kappa}{4m}U_2^2 - \frac{\omega_{r1}^2 - \omega_{n1}^2}{2}\right| = \left|\frac{3\kappa}{8m}U_2^2\right|. \qquad (34)$$

By substitution of the expression for *S2* (given by Eq. (17)) predicts a bifurcation at

$$\omega_{r2}^2 = \frac{3\omega_{n2}^2 - \gamma\omega_{n1}^2}{3-\gamma} \qquad U_2^2 = \left(\frac{2m}{3}\right)\frac{\omega_{n2}^2 - \omega_{n1}^2}{\kappa - 4\kappa_2} \qquad (35)$$

This is same point which is obtained by intersecting Eqs. (25) with Eq. (17) (see Eq. (27)). It is also found that below this bifurcation *S2* is stable, and above it is unstable.

To further verify this result, the stability of the solution has been evaluated numerically using the numerical continuation software AUTO-07p, as discussed in [21]. The software determines the stability of the branches of the backbone curves using Floquet theory, see for example [22]. The condition for

the stability of a periodic orbit is that all Floquet multipliers have a modulus no greater than one. The stability of the other branches have also been determined.

Figure 3(a) shows the *S2* backbone curve along with the $S3^+$ and $S3^-$ branches that bifurcate from it. *S1* has been omitted as a trivial case here, as it is stable throughout. The stable section of the *S2* branch is denoted by $S2_s$, and the unstable section by $S2_u$. Of the four Floquet multipliers associated with the undamped system, two are always unity. The paths of the other two, non-unity, multipliers are tracked as amplitude X_1 increases and the locus of the solutions are shown in Figure 3(b). At $X_1 = 0$, the two non-unity Floquet multipliers are indicated by markers $\times$ and sit on the unit circle (indicated by grey dotted curve). As X_1 increases, the solution follows the $S2_s$ backbone curve which also sits on the unit circle, and hence is neutrally stable. As we reach the bifurcation point, the Floquet multipliers both become unity. From here there are two possibilities: (i) staying on *S2*, the multipliers follow the real axis with one having modulus greater than one, hence stability is lost (labeled $S2_u$); (ii) from the bifurcation point, following the $S3^+$ or $S3^-$ branches, the Floquet multipliers stay on the unit circle as shown by the grey lines and therefore remain neutrally stable.

From this, and using bifurcation theory for Hamiltonian systems, in the displacement amplitude projection this is a pitchfork bifurcation [3,5].

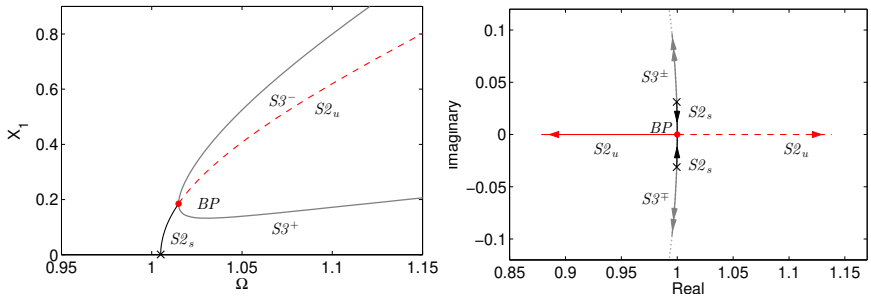

Fig. 3: The stability of the *S2*, $S3^+$ and $S3^-$ backbone curves for the system where $\kappa_2 = 0.05$: (a) the backbone curves; (b) the paths of the two non-unity Floquet multipliers as the amplitude of response increases from zero (marked as $\times$). Note the other two Floquet multipliers are equal to 1 throughout, and so do not affect the stability.

4 Discussion

The backbone curves play an important role in determining the response of the system to an external forcing. Here, a brief example of the relationship between the forced response and the backbone curves is provided. The system

is forced in the second mode, such that $[P_{m1},\ P_{m2}] = [0,\ 6] \times 10^{-3}$, and a damping ratio of $\zeta = 0.004$ is considered.

The forced response has been computed from an initial steady state solution, found with numerical integration in MATLAB. This was then continued in forcing frequency using the software AUTO-07p [23].

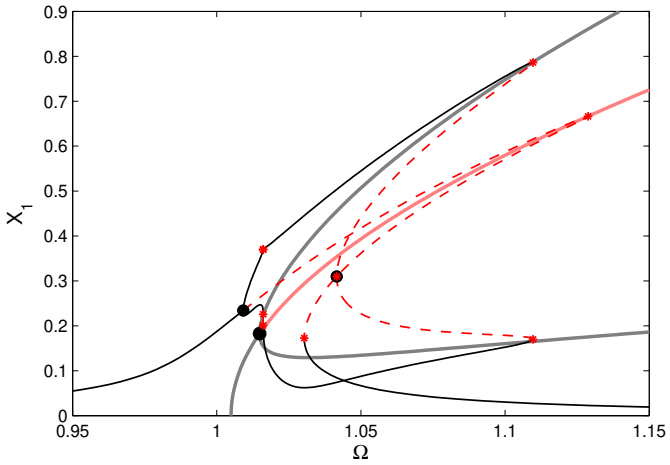

Fig. 4: Displacement amplitude of the first mass when the system is forced in only the second mode (i.e. $[P_{m1},\ P_{m2}] = [0,\ 6]\times10^{-3}$) with damping $\zeta = 0.004$ for both modes. Other system parameters: $\omega_{n1} = 1$, $\omega_{n2} = 1.005$, $\kappa = 0.4$ and $\kappa_2 = 0.05$. The black dots mark the bifurcation of the second-mode-only forced response curve and the red asterisks indicate fold points. The thick grey and red lines represent the stable and unstable backbone curves respectively. Note that as forcing is in the second mode here, *S1* (containing mode 1 only) is not followed, and hence has not been plotted.

Figure 4 shows the displacement of the first mass, X_1, for the system whose backbone curves are presented in the right column of Figure 2. The familiar shape of the response of a Duffing oscillator can be seen following the *S2* backbone where the response is also confined to just the second mode. On this curve there are two bifurcation points, indicated with black dots. The additional curves leading off these points are responses composed of both the first and second resonant responses. It can be seen that their underlying dynamics are captured by the $S3^+$ and $S3^-$ backbone curves. As with the branch attracted to *S2*, these responses cross the *S3* branch in the immediate vicinity of a fold point. Details of the relationship between backbone curves and forced responses are beyond the scope of this work. Nevertheless, the method and findings presented in this work are able to offer a new perspective with which to further the understanding of this process.

5 Conclusions

This work has demonstrated the use of the second-order normal form method for the computation of backbone curves. We have shown that the application of the method to the unforced, undamped equivalent of a system provides time-independent, analytical expressions describing the backbone curves. These expressions can be used to relate the physical properties of the system to characteristics of its behaviour. The backbone curves also provide a simple, graphical representation of the resonant behaviour of the system. Furthermore it has been shown that internal resonances of the system can be related to bifurcations of the backbone curves. We have also demonstrated how these results may be used to determine the stability of the backbone curves and predict the existence and location of bifurcations.

In comparison to previous work, this presents a more general formulation with an approach that may be extended to a variety of models with a higher number of degrees-of-freedom. This method also allows us to quantify phase dependence between the backbone curve solutions and to highlight the existence of internal resonances in the response. The expressions obtained in the application to a 2DOF system agree with the results found by Lewandowski. Furthermore this approach has been validated by a comparison with the solutions obtained via numerical continuation: the maximum deviation between the two predictions is less than 0.1% – as a result of the assumptions made in the formulation of the method.

A forced response for this system was also computed and superimposed with the relevant backbone curves. Due to the correlation between the backbone curves and the forced response, a simplified, analytical interpretation of the complex behaviours of the system is provided. This particular aspect will be the subject of further investigation in future work.

References

1. Arnold, V.I., Levi, M., Szücs, J.: Geometrical Methods in the Theory of Ordinary Differential Equations. Ch. 3, Springer, New York, (2012)
2. Cartmell, M.: Introduction to Linear, Parametric and Nonlinear Vibrations. Ch. 4, Chapman and Hall, (1990)
3. Guckenheimer, J., Holmes, P.: Nonlinear Oscillations, Dynamical Systems, and Bifurcations of Vector Fields. Ch. 4, Springer, New York, (1983)
4. Nayfeh, A.H., Pai, P.F.: Linear and Nonlinear Structural Mechanics. Wiley, (2008)
5. Thompson, J.M.T., Stewart, H.B.: Nonlinear Dynamics and Chaos. Ch. 7, Wiley, Chichester, (2002)
6. Wagg, D.J., Neild, S.A.: Nonlinear Vibration with Control: For Flexible and Adaptive Structures. Ch. 5, Springer, (2009)
7. Neild, S.A., Wagg, D.J.: Applying the method of normal forms to second order nonlinear vibration problems. Proc. R. Soc. A 467, 1141-1163 (2011)
8. Lewandowski, R.: Solutions With Bifurcation Points For Free Vibration Of Beams: An Analytical Approach. J. Sound Vib. 177, 239-249 (1994)
9. Lewandowski, R.: On beams membranes and plates vibration backbone curves in cases of internal resonance. Meccanica 31, 323-346 (1996)

10. Kerschen, G., Peeters, M., Golinval, J.C., Vakakis, A.F.: Nonlinear normal modes, Part I: A useful framework for the structural dynamicist. Mech. Syst. Signal Pr. 23, 170-194 (2009)
11. Rand, R.H.: Lecture notes on nonlinear vibrations. Dept. Theoretical & Applied Mechanics, Cornell University, Ithaca, NY. http://www.tam.cornell.edu/randdocs (2005)
12. Vakakis, A.F., Manevitch, L.I., Mikhlin, Y.V., Pilipchuk, V.N., Zevin, A.A.: Normal Modes and Localization in Nonlinear Systems. Wiley, New York, (1996)
13. Nayfeh, A.H., Lacarbonara, W. and Chin, C.M.: Nonlinear normal modes of buckled beams: three-to-one and one-to-one internal resonances. Nonlinear Dynam. 18 253-273 (1999)
14. Jezequel, L., Lamarque, C.: Analysis of non-linear dynamical systems by the normal form theory. J. Sound Vib. 149, 3, 429-459 (1991)
15. Touzé, C., Thomas, O., Chaigne, A.: Hardening/softening behaviour in non-linear oscillations of structural systems using non-linear normal modes. J. Sound Vib. 273, 1, 77-101 (2004)
16. Neild, S.A.: Approximate methods for analysing nonlinear structures. In: Wagg, D.J., Virgin, L. (eds.) Exploiting Nonlinear Behavior in Structural Dynamics, pp. 53-109 Springer, Vienna (2012)
17. Neild, S.A., Wagg, D.J.: A generalized frequency detuning method for multidegree-of-freedom oscillators with nonlinear stiffness. Nonlinear Dynam. 73, 649-663 (2013)
18. Nayfeh, A.H.: Method of Normal Forms. Wiley, New York (1993)
19. Vakakis, A.F., Rand, R.H.: Normal modes and global dynamics of a two-degree-of-freedom non-linear systemI. Low energies. Int. J. Nonlinear. Mech. 27, 861-874 (1992)
20. Xin, Z.F., Neild, S.A., Wagg, D.J., Zuo, Z.X.: Resonant response functions for nonlinear oscillators with polynomial type nonlinearities. J. Sound Vib. 332, 1777-1788 (2013)
21. Lust, K.: Improved numerical Floquet multipliers. Int. J. Bifurcat. Chaos 11, 2389-2410 (2001)
22. Chicone, C.: Ordinary Differential Equations with Applications. Springer, (2006)
23. Doedel, E.J., Champneys, A.R., Fairgrieve, T.F., Kuznetsov, Y.A., Dercole, F., Oldeman, B.E., Paffenroth, R.C., Sandstede, B., Wang, X.J., Zhang, C.: AUTO-07P: Continuation and Bifurcation Software for Ordinary Differential Equations. Concordia University, Montreal, Canada. http://cmvl.cs.concordia.ca (2008)